MINISTERUL EDUCAŢIEI, CERCETĂRII ŞI INOVĂRII

UNIVERSITATEA TEHNICĂ
DIN CLUJ-NAPOCA

FACULTY OF ELECTRICAL ENGINEERING

Eng. Alina Cristina VIOREL

STUDY ON TRANSVERSE FLUX MACHINE OPERATING AS GENERATOR IN WIND MILLS

ABSTRACT

COORDINATOR

Prof.dr.ing. Ioan-Adrian VIOREL

Table of Contents

I.Introduction

Wind energy is undoubtedly one of the cleanest forms of producing power from a renewable source. There is no pollution, there is no burning of fossil fuels and the electricity is made by kinetic power of the wind.

Small wind turbines are used for wind farms essentially and the installed power can vary in number from one to hundreds of turbines and generate power to as much as to several hundred megawatts.

Various wind turbine concept have been developed and built to maximize the energy harnessed, to minimize the cost, and to improve the power quality during the last two decades. Such turbine concepts can be classified with a view to the rotational speed, the power regulation, and the generator system.

The advantage of using direct drive energy converter is that it omits the gearbox in the system, decreases the part count and operates at lower speed therefore has reduced wear and tear. The permanent magnet generator represents an excellent choice in direct drive systems for producing clean energy.

In this paper is proposed a simplified layout of transverse flux machine, for small wind turbine. A main part of the present work is done for integration the structure into models which exists already in literature. Thus, numerical and analytical approaches are adapted accordingly to the proposed structure.

The thesis has 8 chapters. In Chapter I is made a general presentation and is explained the main purpose of choosing this subject. The second chapter is dedicated to a general overview regarding different types of wind turbines, their features and for criteria used in designing a wind turbine.

The simplified mathematical model is based on some magnetic equivalent circuits, fully described in the Chapter III, which allows for the calculation of the main no-load flux, permanent magnet leakage fluxes, for the sizing magnets permanents and computer simulation of the generator steady state and dynamic behavior. A verification of the machine model by using Flux3D environment from CEDRAT is done. Chapter IV contains a specific designing algorithm (sizing equations, permanent magnet calculation, iron core sizing, losses in iron core, magnets and winding) for transverse flux generator. A thermal model is developed for transverse flux generator. The scaling procedure applied for designing a transverse flux machine family is presented and a comparison between scaling and designing is done in the end. In chapter V is given a comparison between one phase and three phase generators. Different variants of the transverse flux generator base modules are designed. Using the Matlab/SIMULINK platform is present a wind mill system model (including energy storage system model) in Chapter VI. In Chapter VII the developed experimental model, is presented together with some tests results. The identification of the Lundel generator equivalent circuit generator parameters are made, which allows for a full comparison between the simulation results and tests for the wind mill model.

Finally, conclusions and contributions, glossary, bibliography and appendices are to be found.

III. Rotational Transverse Flux Machine

The transverse flux machine, in both its variants, with or without permanent magnet excitation, tends to become a mature machine with a well defined application domain - the low speed, high torque density drives. A new comer in its modern construction, supply and control, the permanent magnet transverse flux motor (PMTFM) has an achievable torque density two times larger than that of conventional or tooth-wound winding permanent magnet synchronous motors [W4, V4, H16, W1].

The PMTFM has a particular structure. Each phase is an independent module with a single armature winding, of circular shape. Even if PMTFM behaves as a PM synchronous motor, its structure is very different. In order to design and study the PMTFM, a very specific model should be developed, and a three dimensions finite element method (3D-FEM) has to be employed. Some attempts to develop a useful design procedure and to define an adequate mathematical model were made [S1, A3, A4, and V9], most of them being dedicated to a conventional PMTFM structure, with claw poles in stator and were combining the 3D-FEM analysis results with analytical calculations.

The PMTFM has three main breakpoints: small power factor (inherent to larger torque density), partial PM utilization and a complicated structure. The small power factor is related to high torque density via high pole **mmf** and also to PM flux fringing (leakage); it can be improved, though incrementally, by reducing the latter via improved rotor topologies.

Having a reduced price and simple technology, the structure proposed in this paper is derived from a reluctance topology. The only important change is made in the rotor, where a permanent magnet (PM) is introduced between the two poles of each pole piece. Thus, from elementary reluctance topology with the same number of stator and rotor poles, presented in Fig. 3.18, the new structure obtained is presented in Fig. 3.19, introducing in every rotor poles permanent magnets with alternative polarization (the number of rotor poles becomes double compared with stator one). One phase structure of the proposed motor is presented in Fig. 3.19, where a linear layout is depicted.

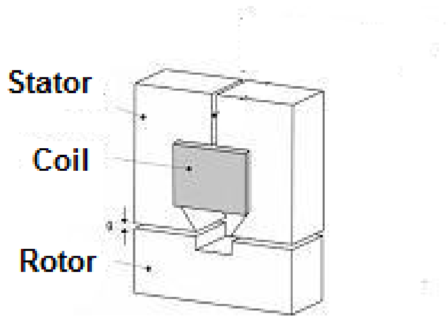

Fig.3.18 Stator and rotor poles for a TFRM.

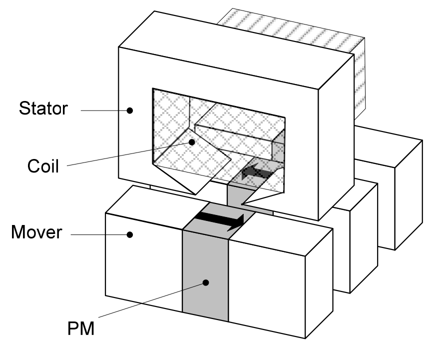

Fig. 3.19 PMTFM, novel structure, phase module in linear layout.

The generator iron core can be made out of steel laminations or soft magnetic composite (SMC) materials. The rotor poles of the proposed PMTFG should be made out of SMC materials, since it allows a 3D flux pattern. The stator core can also be made of SMC due to the less complicated construction technology. In the case of SMC, the initial permeability and the saturation are smaller than that of a good steel lamination.

3.3.2 Analytical model based on equivalent magnetic circuits

The magnetic equivalent circuits are constructed for different situations, in order to calculate the no-load main flux, the armature reaction flux and the most important leakage fluxes. In the case of no load fluxes, when there is no current in armature winding, the magnetic equivalent circuit considered, one rotor pole piece in aligned position, is the one given in Fig.3.3.4.

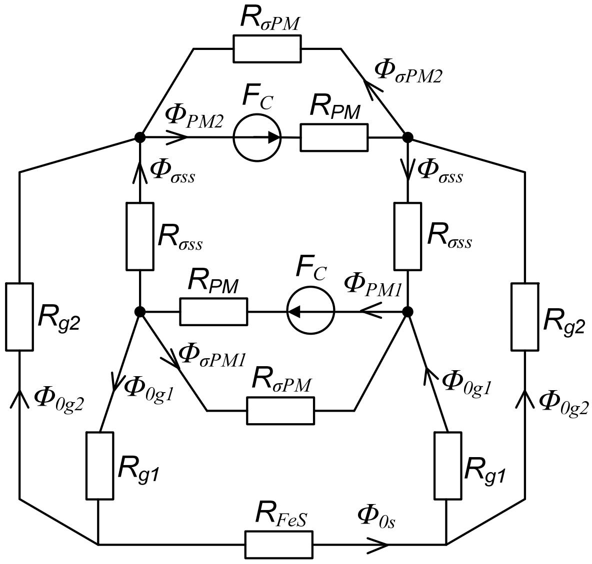

Fig.3.3.4 No load PMTFG magnetic equivalent circuit.

The following notations are used:

- Φ_{0g1}, Φ_{0g2} - no-load air-gap main fluxes
- $\Phi_{\sigma ss}$ - side to side leakage flux (Fig.4)
- $\Phi_{\sigma g}$ - air-gap leakage flux (Fig.5)
- $\Phi_{\sigma s}$ - side pole leakage flux (Fig.4)
- $\Phi_{\sigma b}$ - rotor pole bottom leakage flux (Fig.5)
- R_{PM}, $R_{\sigma ss}$, $R_{\sigma g}$, $R_{\sigma s}$, $R_{\sigma b}$ - reluctances corresponding to the Φ_{PM}, $\Phi_{\sigma ss}$, $\Phi_{\sigma g}$, $\Phi_{\sigma s}$, $\Phi_{\sigma b}$ fluxes
- R_{g1} - air-gap reluctance under rotor pole in aligned position, (pole 1 in Fig.6)
- R_{g2} - air-gap reluctance under the unaligned rotor pole, (pole 2 in Fig.6)
- R_{FeS} - one stator pole piece reluctance
- $F_C = H_C \cdot l_{PM}$, where H_C is the PM's coercitive field value and l_{PM} the PM's length

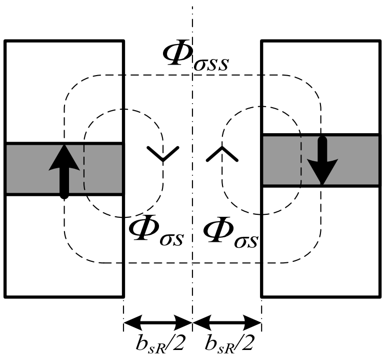

Fig.3.3.1. Rotor pole, side and side to side leakage flux

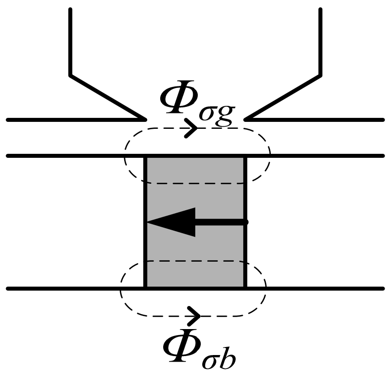

Fig.3.3.2. Rotor PM's air-gap and bottom leakage flux

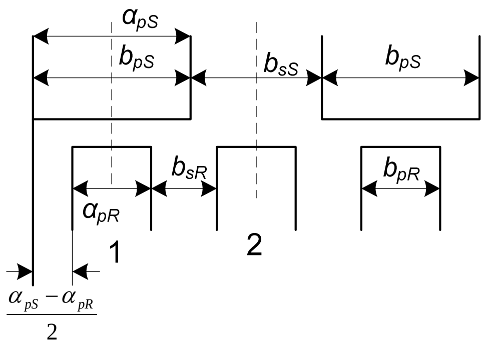

Fig.3.3.3. Air-gap configuration in aligned rotor position

In the magnetic equivalent circuit given in Fig.3.3.4, the considered own leakage fluxes of one PM presented in Figs.3.3.1&3.3.2, are substituted by an equivalent flux, the reluctances' equivalence being given in equation (3.3.2).

$$\frac{1}{R_{\sigma PM}} = \frac{1}{R_{\sigma g}} + \frac{1}{R_{\sigma s}} + \frac{1}{R_{\sigma b}} \tag{3.3.2}$$

where the reluctances $R_{\sigma g}$, $R_{\sigma s}$ and $R_{\sigma b}$ correspond to the fluxes $\Phi_{\sigma g}$, $\Phi_{\sigma s}$ and $\Phi_{\sigma b}$.

The magnetic equivalent circuit given in Fig.3.3.4, for zero armature current, does not contain a magnetic reluctance corresponding to the rotor pole, but it can be introduced, and also the core nonlinearity can be taken into consideration.

The machine poles' configuration is given in Fig.3.3.3, one rotor pole being in aligned position, the initial position considered for air-gap reluctances, R_{g1} and R_{g2} calculation.

The magnetic equivalent circuit constructed to calculate the armature reaction flux with a rotor pole piece in aligned position, respectively with the rotor pole pieces in unaligned position are given in Figs.3.3.9, 3.3.10. In the magnetic equivalent circuit from Fig.3.3.10, due to the perfect rotor symmetry, the Φ'_{Sgun} is considered half of the total stator flux produced in unaligned position Φ_{Sgun}.

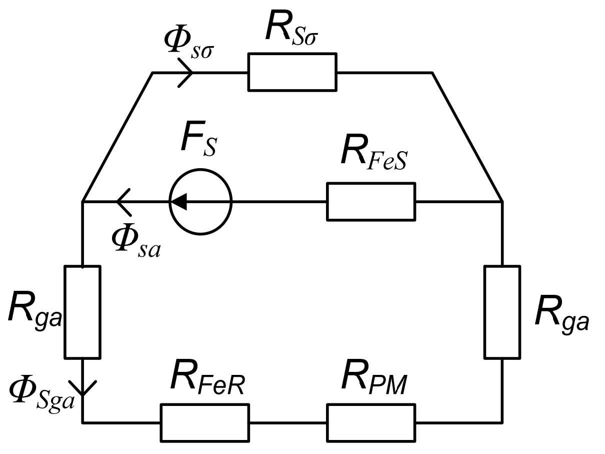

Fig.3.3.9 Magnetic equivalent circuit, armature reaction rotor pole piece in aligned position

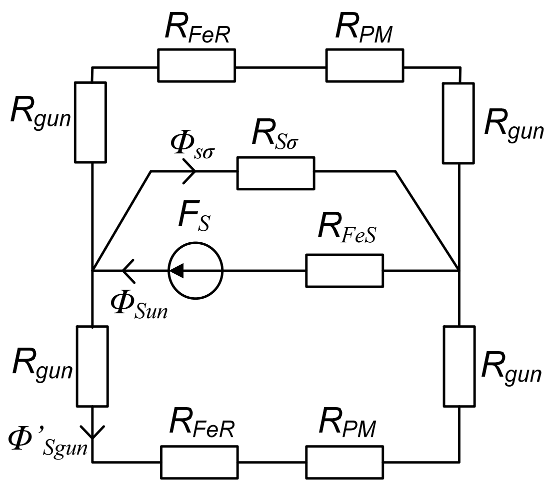

Fig.3.3.10. Magnetic equivalent circuit, armature reaction, rotor pole pieces in unaligned position

In both magnetic equivalent circuits, Figs 3.3.9, 3.3.10, the total stator windings leakage reluctances, $R_{\sigma s}$ is defined as:

$$R_{s\sigma} = \frac{R_{\sigma sl} \cdot R_{\sigma a}}{R_{\sigma sl} + R_{\sigma a}} \tag{3.3.13}$$

where $R_{\sigma sl}$ and $R_{\sigma a}$ are the slot leakage and respectively the air leakage reluctances associated to the slot leakage flux $\Phi_{\sigma sl}$ and air leakage flux $\Phi_{\sigma a}$, which is circling the stator winding in the air portion between two consecutive stator pole pieces.

The signification of the notations made in Figs.3.3.9 and 3.3.10 are the following:

Φ_{Sa}, Φ_{Sun} – stator flux in aligned, respectively unaligned rotor position

Φ_{Sga}, Φ_{Sgun} – air-gap flux in aligned, respectively unaligned rotor position

$F_S = NI$ – stator phase **mmf** (N – phase number of turns, I – phase current)

R_{ga}, R_{gun} – air-gap reluctance under a rotor pole in aligned, respectively unaligned position

R_{FeS}, R_{FeR} – stator and rotor pole reluctances

R_{PM} – permanent magnet reluctance

The aligned air-gap flux, Φ_{Sga} is given by the equation:

$$\Phi_{Sga} = \frac{F_S}{\left(2R_{ga} + R'_{PM}\right)\left(1 + R_{FeS} / R_{S\sigma}\right) + R_{FeS}} \tag{3.3.16}$$

where R'_{PM} represents the sum of PM and rotor pole reluctance:

$$\frac{1}{\Re_{\sigma PM}} = \frac{1}{\Re_{\sigma s}} + \frac{1}{\Re_{\sigma g}} + \frac{1}{\Re_{\sigma b}} \tag{3.3.2}$$

The unaligned air-gap flux, Φ_{Sgun} is:

$$\Phi_{Sgun} = \frac{F_S}{0.5\left(2R_{gun} + R'_{PM}\right)\left(1 + R_{FeS} / R_{S\sigma}\right) + R_{FeS}} \tag{3.3.15}$$

The armature reaction fluxes ratio is considered equal to the main inductance ratio:

$$\Phi_{Sga} / \Phi_{Sgun} = M_d / M_q \tag{3.3.24}$$

The stator phase leakage inductance is:

$$L_\sigma = \mu_0 Q_S N^2 \left(P_{sl} b_{pS} + b_{sS} \frac{ln(1.5)}{2\pi} \right) \tag{3.3.26}$$

where the slot leakage permeance P_{sl} is:

$$P_{sl} = \frac{h_s}{3w_s} + \frac{h_0}{w_s - l_0} ln\left(\frac{w_s}{l_0}\right) \tag{3.3.20}$$

Q_S is the number of stator pole pieces, b_{pS} and b_{sS} are the stator pole, respectively inter pole length, h_s and l_o are the slot height, respectively opening part of the stator, unoccupied by conductors.

The no-load induced **emf** maximum value can be calculated with the flux Φ_{0s} obtained by solving the magnetic equivalent circuit given in Fog.3.3.4, the same flux allowing for electromagnetic torque calculation.

Supposing that the resulting no-load air-gap flux density varies sinusoidal, its maximum value being B_{gmax}, the peak value of the cogging torque produced by one phase module is estimated by:

$$T_{cg\,max} = Q_S^2 \frac{g \cdot B_{g\,max}}{\mu_0} \tag{3.3.49}$$

where g is the actual air-gap length.

In order to avoid the PM's demagnetization process, the air-gap flux produced by PM in aligned rotor position must be greater than the air-gap flux produced by stator **mmf** in the same rotor position,

$$\Phi_{0ga} > \Phi_{Sga} \tag{3.3.32}$$

From (3.3.32) results a condition for the minimum PM's length to avoid its demagnetization once all other dimensions are given.

3.4. The checking of the analytical model through the FEM analyses.

In order to check the analytically obtained results, a three dimensions finite element method (3D-FEM) analysis was employed. Due to PMTFG symmetry, only two rotor and one stator pole pieces were modelled in a manner that allows automatic re-meshing at different rotor position. A 3D-FEM package from CEDRAT was used and a bunch of results were obtained. Two support planes were constructed in the model, at midway between two neighbouring pole pieces and in the radial middle plane pf the PMs, more details being given in [S6], in order to calculate the PM's main and leakage fluxes. All the calculation were done for a 1.2kW, 300rpm PMTFG with 15 stator pole pieces and an average air-gap diameter D_g = 0.161m. The stack length for one module is L = 0.038m, and the PM's axial length is l_{PM} = 0.008m. Both the stator and the rotor cores are made of SOMALOY500 with absolute permeability μ_{Fe} = $6.283 \cdot 10^{-4}$H/m. A comparison between analytically and 3D-FEM analysis results for the no-load fluxes are given in Table 3.4.1.

Table 3.4.1. The no-load fluxes [10^{-4} Vs]

Flux	ϕ_{PM1}	ϕ_{0g1}	ϕ_{PM2}	ϕ_{0g2}	ϕ_{0S}	$\phi_{\sigma ss}$
Analytical	2,34	1,3	1,6	0,6	0,7	0,9
3D-FEM	2,0	1,1	1,7	0,7	0,4	0,7

The differences look impressive, mainly in the case of $\Phi_{\sigma ss}$, but, to separate this one from other PM's leakages is quite difficult, and even the 3D-FEM results might contain some errors. It is obvious, as shown in [S6], that the side to side leakages, $\Phi_{\sigma ss}$ are larger than the air-gap flux for the shifted second rotor pole, and they must be reduced by decreasing the side rotor pole area or by employing anti-Hallbach arrays [S6].

Electromagnetic torque peak value for the same sample PMTFG and square rotor pole side area is 18.2Nm from the 3D-FEM analysis results, respectively 18.617Nm via analytical calculation. The peak value of the cogging torque is 6.8Nm via 3D-FEM and 5.994Nm by analytical method. These values evince the fact that the simplified proposed model is satisfactory covering the phenomena. By using the simplified model, a sizing design procedure can be developed easily and some interesting results can be obtained.

The influence of the iron core material, high quality steel slides or SMC, or of the PMs' dimensions on the PMTFG performances can be studied too using the analytical model, together with the influences of many other factors as ratio or average air-gap diameter to stack length (the aspect factor).

5.4. Different designed variants for the transverse flux generator base module.

The base module variants have the found with a rated power of 8 kW and 11 respectively. The different designed variants have different number of poles, different rotational and different dimensional coefficients. One example for dimensioning is presented in Tables 5.4.1 and 5.4.2. The data sheet are for a transverse flux generator with rated power of 8 kW, 30 stator rotor poles and rotational speed between 2 and 4 rot/sec. The tables contain several information such as output values, and main dimensions for two variants of iron core material (steel laminations and SMC respectively)

Tabelul 5.4.1. Transverse flux generators of 8kW, Q_S = 30, outside values.

Gen.	n [1/s]	permea bility	E [V]	T_p [Nm]	P [kW]	L_σ [H] *e-5	M_d [mH]	M_q [mH]	denT [Nm/ kg]	η	ΔT_{emp} [°C]
1G8230	2	500	240	639	8,031	11,72	12	10	8,65	0,889	25,09
		2800	239	637	8,006	10,69	11	10	8,60	0,891	24,73
1G8330	3	500	240	426,8	8,046	8,755	8,009	7,231	7,64	0,901	26,7
		2800	239	424,8	8,009	7,928	7,577	6,987	7,6	0,902	26,4
1G8430	4	500	239	319,8	8,022	6,974	6,158	5,529	6,86	0,907	28,01
		2800	241	321,7	8,085	6,501	5,899	5,419	6,9	0,908	28,04

Tabelul 5.4.2. Transverse flux generators of 8kW, Q_S = 30, main dimensions.

Gen.	n [1/s]	permea bility	N_t	D_g [m]	L [m]	l_{pR} [m]	b_{pR} [m]	b_{pS} [m]	l_{PM} [m]	h_{PM} [mm]	w_s [m]	h_s [m]
1G8230	2	500	67	0,345	0,069	0,031	0,013	0,025	7,67	0,040	0,015	0,094
		2800	64	0,345	0,069	0,031	0,013	0,025	7,4	0,040	0,015	0,094
1G8330	3	500	62	0,301	0,06	0,027	0,011	0,022	7,11	0,034	0,015	0,094
		2800	60	0,301	0,06	0,027	0,011	0,022	6,82	0,034	0,015	0,094
1G8430	4	500	58	0,274	0,055	0,024	0,010	0,020	6,37	0,031	0,015	0,094
		2800	56	0,274	0,055	0,024	0,010	0,020	6,46	0,031	0,015	0,094

Some results are presented in Figs.5.4.1, 5.4.2

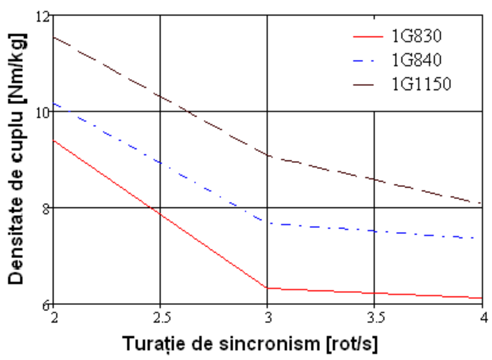

Fig.5.4.1 The density torque variation to the rotational speed

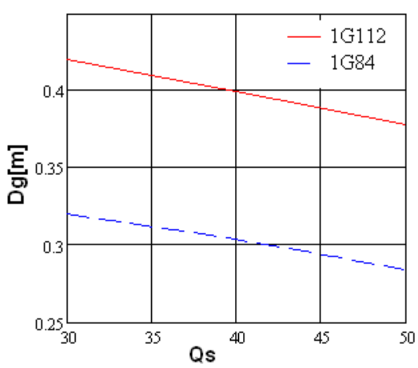

Fig.5.4.2 Diameter variation to the polar pieces number

The computed values are:

- maximum induced EMFf E[V];
- torque per Tp [Nm];
- leakage induction L_σ [H];
- the leakage induction d,q - parameters M_d and M_q [H];
- torque density denT [Nm/kg];
- the efficiency η;
- the increasing temperature rated to 40ºC;

The main dimensions are:

- the air-gap diameter D_g [m];
- rotor length L[m];
- rotor pole width b_{pR} [m];
- stator pole width b_{pS} [m];
- magnet permanent length l_{PM} [m];
- magnet permanent height h_{PM} [m];
- slot width w_s [m];
- slot height h_s [m];

6. Features of the wind turbine equipped with transverse flux generator for small wind turbines.

A small wind turbine could be equipped with a transverse flux generator for a small power wind mill. The system has no gearbox and the main structure is presented in Fig. 6.1.1.

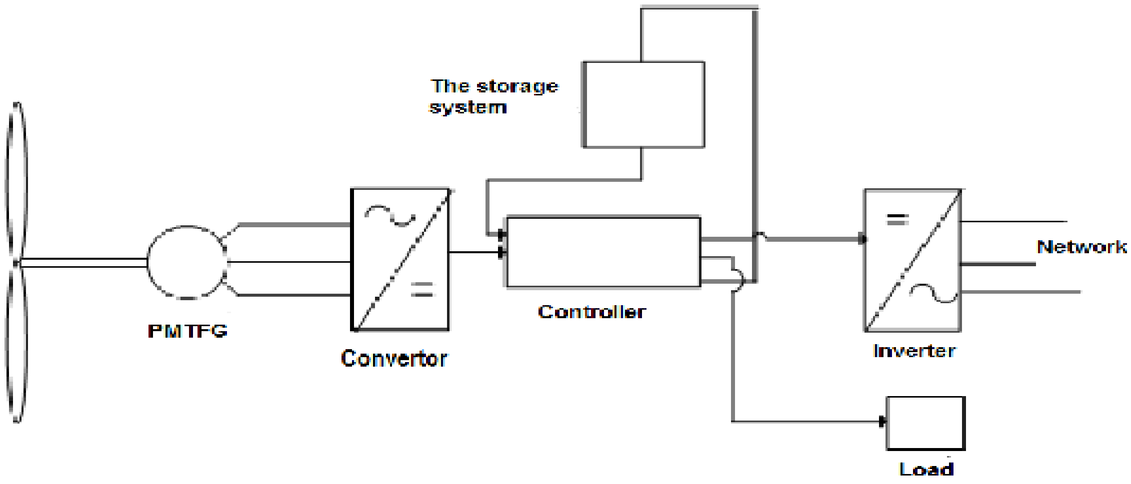

Fig.6.1.1. Wind turbine structure

The wind gust used in the application is predetermined one and the shape is presented in Fig. 6.2.9. The wind turbine answer is presented in Fig.6.2.10.

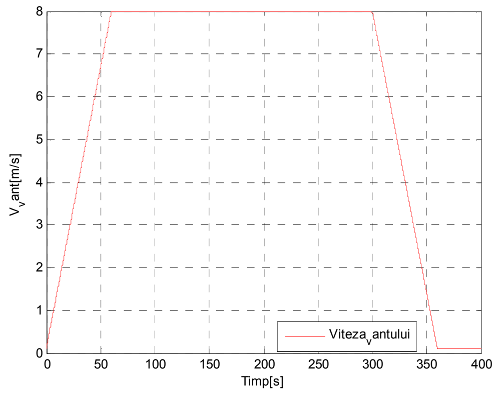

Fig. 6.2.9. The shape of the considered wind gust.

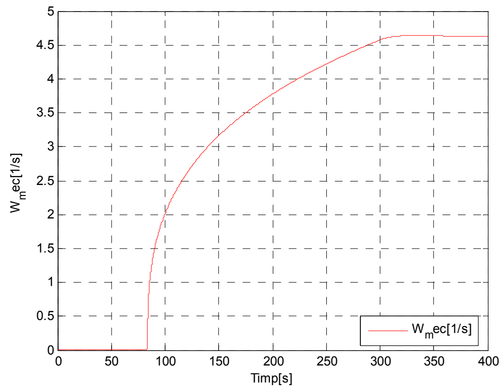

Fig. 6.2.10. the answer of the wind turbine

In Fig.6.4.3, 6.4.4 and 6.4.5 the results presented considering different situations, like introducing a filter in the system.

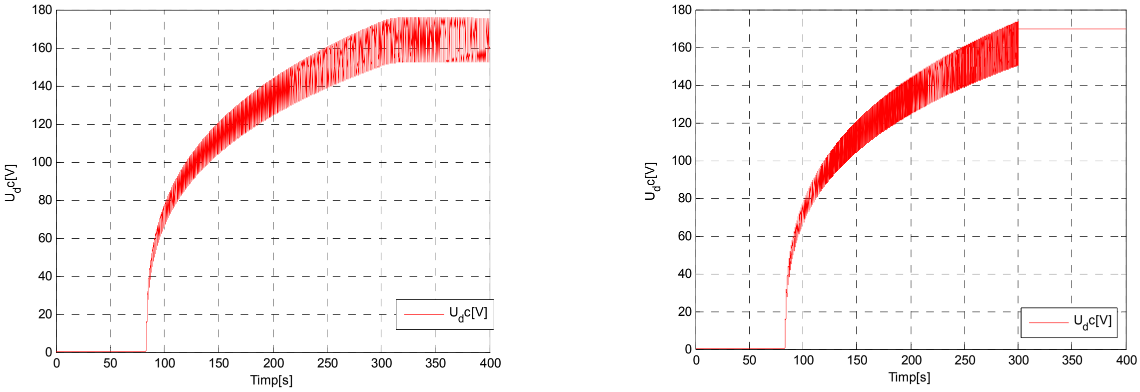

a) b)

Fig. 6.4.3. a, b. The convertor voltage variation without and with filter.

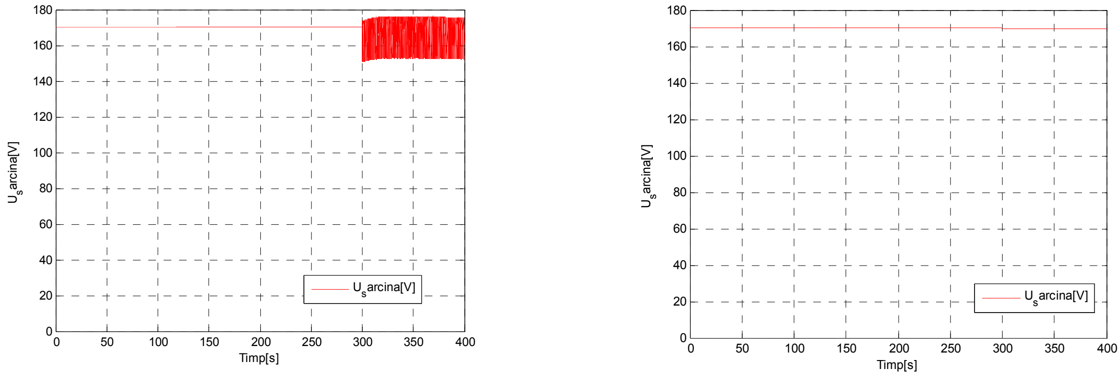

a) b)

Fig. 6.4.4, a, b. The load voltage variation without and with filter.

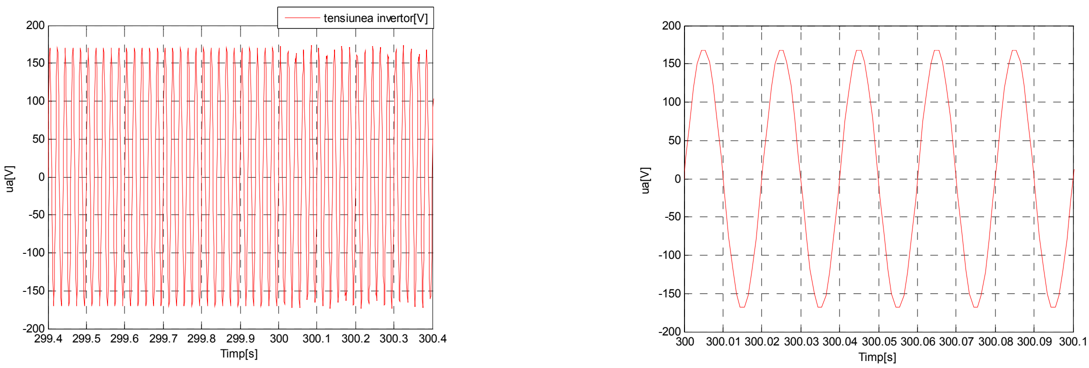

a) b)

Fig. 6.4.5. a), b The inverter voltage variation without and with filter

8. Contributions.

Some important aspects need to be named:

- A transverse flux generator simplified structure was proposed in the paper for wind turbines applications;
- An analytical model in developed allowing for all fluxes computations and for dimensioning the permanent magnet;
- Developing a thermal model of the generator;

- Scaling procedure used for designing transverse flux machine;
- Different designed variants for the transverse flux generator base module;
- Creating in Matlab/SIMULINK a wind mill system model;
- Developing a laboratory wind mill model.

References (selection)

A3 ARSHAD, W.M., BACKSTRÖM, T., SANDRAGANI, C. - “Analytical design and analysis procedure for a transverse flux machine”, Proc.of IEMDC’01, Cambridge, MA, USA, 2001, pp. 115-121.

A4 ANAPALAHAN, P. - “Design of transverse flux machine using calculations and finite element analysis”, Master Thesis, Royal Institute of Technology, Stockholm, 2001.

D2 DUBOIS, M.R. - “Optimized permanent magnet generator topologies for direct-drive wind turbines”, PhD Thesis, Technical University of Delft, Holland, 2004.

H3 HENNEBERGER, G., BORK, M. - "Development of a new transverse-flux motor", Electromotion, vol.5, no.1, 1998, pp.1-8.

H16 HENNERBERGER, G., VIOREL, I.A. – “Variable reluctance electrical machines”, Shaker Verlag, Aachen, 2001.

I2 IOV, F., HANSEN ANCA D., SØRENSEN, P., BLAABJERG, F. - “Wind Turbine Blockset in Matlab/SIMULINK, General overview and description of the models”, Institute of Energy Technology Aalborg University, March 2004, ISBN 87-89179-46-3.

O1 ONG, C.M. - „Dynamic simulation of electric machinery using Matlab/Simulink”, Prentice Hall PTR, Upper Saddle, 1998.

S1 STRETE LARISA, VIOREL, I.A., VIOREL ALINA - “On the designing procedure of a permanent magnet transverse flux generator (PMTFG) with specific topology, 11th International Conference on Optimization of Electrical and Electronic Equipment Optim’08, Braşov, 2008, pp.99-104.

S6 STRETE LARISA, VIOREL I.A., BOLDEA, I. – “Studies on the performance of permanent magnet transverse flux motors with a particular rotor topology” ISEF’09, Arras, France, Sept., 2009, on CD-ROM, vol.of Digests, pp.101-103.

V1 VIOREL, I.A., STRETE LARISA, VIOREL ALINA - "Steady state simplified mathematical model of a particular permanent magnet transverse flux motor", ISEF’09, Arras, France, Sept., 2009, on CD-ROM, vol.of Digests pp.97-99.

V2 VIOREL ALINA, PANU, M. - “A scaling procedure based designed method for a transverse flux motor”, Proc. Of EDPE 2005 13th International Conference on Electrical Drives and Power Electronics, Dubrovnik, Croatia, pp. 65-69.

V3 VIOREL, I.A., VIOREL Alina - "Transverse flux generator based wind mill – a solution for small power stand-alone systems”, National Colloquium on Electrotechnologies and the environmental, Sibiu, 2004, on CD-ROM.

V5 VIOREL, I.A., HENNERBERGER, G., BLISSENBACH, R., LÖWENSTEIN, L. - “Transverse flux machines. Their behavior, design, control and applications” Mediamira Publ. House, Cluj, Romania, 2003.

V9 VIOREL, I.A., BLISSENBACH, R., HENNERBERGER, G., POPAN, A. - “The transverse flux motor mathematical model”, Revue Roum. Scie.Tech., Electrotechn. Et. Energ. Vol.48, no.2-3, pp.369-379, 2003, Bucharest, Romania.

V10 VIOREL, I.A., STRETE LARISA - “A simple modular permanent magnet transverse flux generator”, Proc.of. PCIM China, Sanghai 2008, pp.242-247.

V10 VIOREL, I.A., STRETE LARISA - “A simple modular permanent magnet transverse flux generator”, Proc.of. PCIM China, Sanghai 2008, pp.242-247.
W1 WEH, H., HOFFMANN, H., LANDRATH, J. - "New permanent magnet excited synchronous machine with high efficiency at low speeds", Proc. of ICEM'88, Pisa, Italy, pp.1107-1111.
W2 WEH, H. - "Synchronous machines with new topologies", Proc. of Int. Conf. on the Evolution and Modern Aspects of Synchronous Machines, Zurich, 1991, pp.C1-C8.
W4 WEH, H., JIANG, J. – “Berechnungsgrundlagen für Transversalflussmaschinen”, Archiv f. Elektrotechnik, vol.71, 1988, pp.187-198.